

Appendix from J. P. Drury et al., “A General Explanation for the Persistence of Reproductive Interference” (Am. Nat., vol. 194, no. 2, p. 268)

Supplementary Methods

Early and Late Season Visits

At one site (La Palma; table A1), we conducted experiments during two different time periods—once in the early season, when *Hetaerina titia* males and females exhibit light-phase phenotypes similar to those of *Hetaerina occisa*, and once in the late season, after the population of *H. titia* has undergone a dramatic phenotypic shift and has divergent dark-phase phenotypes (see detailed descriptions in Drury et al. 2015a, 2015b). Thus, for our analyses of pairwise similarity between females, we treat these two separate visits as separate sites.

Indexes of Female Wing Similarity

We measured female wing lightness using photographs of females that were used in tethering experiments from each site. For sites where fewer than 25 photographs of tethered females were available, we added photographs of other females from the site to reach a sample size of 25 where possible. Overall, we measured photographs of 1,101 females (mean \pm SD per species per site = 32.28 ± 20.03 , $n = 16$ sites). Following an established protocol (Drury et al. 2015b), we measured the RGB profile for the basal and distal halves of both wings in color-balanced photos, for a total of four measurements on each photograph. From these photographic measurements, we generated four site-level indexes of female wing similarity (table A2).

At a subset of sites, we also used reflectance spectroscopy to quantify the lightness of female wings. For sites where heterospecific females came from translocation experiments, we used the reflectance values from the site of origin for females. In one case, we used reflectance measurements from a nearby site (Castroville) rather than the site of origin (San Jacinto), as there was no difference in the photographic index of lightness between these two sites (Wilcoxon rank sum test, $W = 211$, $P = .14$, $n_{CV} = 25$, $n_{SJ} = 13$). In total, we scanned 505 females (mean \pm SD per species per site = 20.32 ± 7.87 , $n = 12$ sites). Reflectance measurements were taken at the base, midpoint, and tip of each female’s wing, as described elsewhere (Drury et al. 2015b), using an Ocean Optics USB 200 spectrometer equipped with a fiber-optic reflectance probe (Ocean Optics R200-7-UV-VIS) connected to a pulsed xenon light source (Ocean Optics PX-2).

From these reflectance scans, we used the R package *pavo* (Maia et al. 2013) to calculate the total intensity of each patch as the sum of reflectance values binned at 2-nm intervals. We then generated two reflectance-based indexes of female wing similarity (table A2).

Overall, the photographic measurement of lightness is highly correlated with the log-transformed reflectance-based measurement of lightness (linear regression model, $F_{1,250} = 946.6$, $P < .001$, adjusted $R^2 = 0.79$, $n = 252$ individuals).

Comparative Statistical Analyses

We tested for correlations between pairwise female wing comparisons and reproductive isolation due to male mate recognition (MR) using Spearman’s rank-order correlations. For discriminant function indexes of similarity, each pairwise comparison yields two indexes of misidentification (i.e., the probability that species A is misidentified as species B, and vice versa), so we used all pairwise comparisons in our analyses. However, for the other variables (e.g., Euclidean distance in photographic lightness), the same similarity index applies to both species in the comparison. To account for this nonindependence, we randomized the data by dropping one of each species pair \times site combination and calculating the Spearman’s correlation coefficient (ρ) on this randomized subset. We then repeated this procedure 1,000 times to produce a distribution of ρ values.

In addition to the nonindependence that arises from the pairwise nature of the analysis, we also accounted for the evolutionary nonindependence of taxa in our analyses using a phylogenetic simulation approach (Drury et al. 2015b, 2018). To conduct the phylogenetic correction for correlations of univariate measurements (photographic-based lightness difference and reflectance-based lightness difference), we first fit Brownian motion (BM) and Ornstein-Uhlenbeck (OU) models of trait evolution to the trait data and phylogeny (see “Phylogeny Construction” below) using maximum

likelihood optimization in the R package mvMORPH (Clavel et al. 2015). We then simulated 1,000 data sets using the maximum likelihood parameter estimates from each of these models. For each of these simulated data sets, we ran Spearman's correlations using the simulated index of female wing similarity and the observed values of reproductive isolation to generate a phylogenetically informed null distribution of test statistics. We then compared the observed mean ρ value from the randomization outlined above to this null distribution using one-sample t -tests.

For the discriminant function and overlap variables, we fit multivariate trait models using a recently developed penalized likelihood approach (see `fit_t_pl.R` and associated documentation at <https://github.com/hmorlon/PANDA>) that estimates BM and OU parameters well, even in cases where the number of traits is near to or exceeding the number of tips in a phylogeny (Clavel et al. 2019). As above, we then simulated 1,000 multivariate BM and OU data sets from these model fits. To generate these phylogenetically simulated data sets, for each site we generated a number of samples matching the number of empirical samples (e.g., if there were 25 photos of *Hetaerina americana* females measured at Bonita Creek, we simulated 25 values). We simulated these values with a mean value equal to the mean of the phylogenetically simulated data set and with standard deviation values set to the observed standard deviations of species-level measurements of the empirical data sets. For each site, we then used these simulated data sets to calculate the simulation-based female wing similarity indexes and then ran the correlation tests and comparisons with the empirical ρ values as above.

Phylogeny Construction

We added several new sequences (table A3) to the phylogenetic analyses published previously (Drury et al. 2015b), amplifying the same loci and following the same protocols outlined in that article. From the Bayesian posterior of trees built in MrBayes 3.2.2 (Ronquist et al. 2012) through the Cypres web portal (Miller et al. 2010), we created a maximum clade credibility tree (fig. A2) using TreeAnnotator v. 1.7.4 (Drummond et al. 2012). For all analyses presented here, we trimmed the phylogeny to have one branch for each species and then rendered this pruned phylogeny ultrametric using the `chronos` function in the R package `ape` (Paradis 2011).

Additional Details for Tests for RCD in Male MR

Hetaerina titia exhibits a seasonal polyphenism, wherein individuals emerging in the spring possess light-phase phenotypes similar to those of other congeners and, as a result, engage in higher levels of behavioral interference early in the year (Drury et al. 2015a). For allopatric MR experiments, all trials were conducted in the late season, when divergent dark-phase forms predominate in populations of *H. titia*.

For *H. titia* males, we presented conspecific and *Hetaerina americana* females to *H. titia* territory holders at a sympatric site (Castroville) and at an allopatric site (Burr Ferry). At the sympatric site, we obtained *H. americana* females from the same drainage as the transect. At the allopatric site, we collected live *H. americana* from a site (San Jacinto) 205 km away (30.21°N, -95.40°W). We conducted all female tethering as described in the main text, and nearly all trials were conducted on the same day as the initial collection.

Tests for reproductive character displacement (RCD) in heterospecific male MR were conducted using either translocations of live *H. titia* females or using experimental wing darkening of conspecific females (Drury et al. 2015a, 2015b). Live *H. titia* females were transported to a nearby allopatric site with *Hetaerina occisa* males (once from Otapa to Upper Otapa where we recorded only one *H. titia* male and no *H. titia* females over the course of several visits, once from La Palma to Laguna Escondida where we never recorded any *H. titia* individuals in visits lasting several weeks over a 3-year period). We conducted experimental wing-darkening experiments on *H. americana* in sympatry (Castroville) and allopatry (Lampasas) and on *H. occisa* in sympatry (La Palma) and in allopatry (Cuetzalapan, Laguna Escondida).

To verify the statistical robustness of our results—and, in particular, the finding that interactions between site type and female treatment were not statistically significant—we conducted a permutation test. We randomized the order of female treatment for allopatric populations and reran the regression analyses used in the raw analyses 1,000 times to generate a null distribution of test statistics for the interaction term. We then compared our observed test statistic to this distribution. In all instances, the observed test statistic for the interaction term fell entirely outside of the permuted range (i.e., $P = 0$; fig. A3), indicating that the nonsignificant terms observed in our analyses (table 1; fig. 3) are statistically robust.

Estimating Population Structure in *H. americana*

We used seven previously generated nuclear microsatellites from wild-collected *Hetaerina americana* damselflies (Anderson and Grether 2013). We collected *H. americana* damselflies during the summers of 2004–2012 in the southwest United States and Mexico. This analysis considers 131 individuals from 14 riverine sites (table A6; 6–20 individuals per site). Within a few hours of collection, damselflies were preserved in 95% ethanol. Seven microsatellite loci—h1, h3, h4, h7, h8, h11, and h15—were amplified following the polymerase chain reaction protocol described in Anderson and Grether (2013). Population pairwise differences (F_{ST}) were calculated using GenAlEx v6.0 (Peakall and Smouse 2012). A Mantel's test was performed to examine the correlation between genetic and geographic distances in GenAlEx v6.0 (Peakall and Smouse 2012).

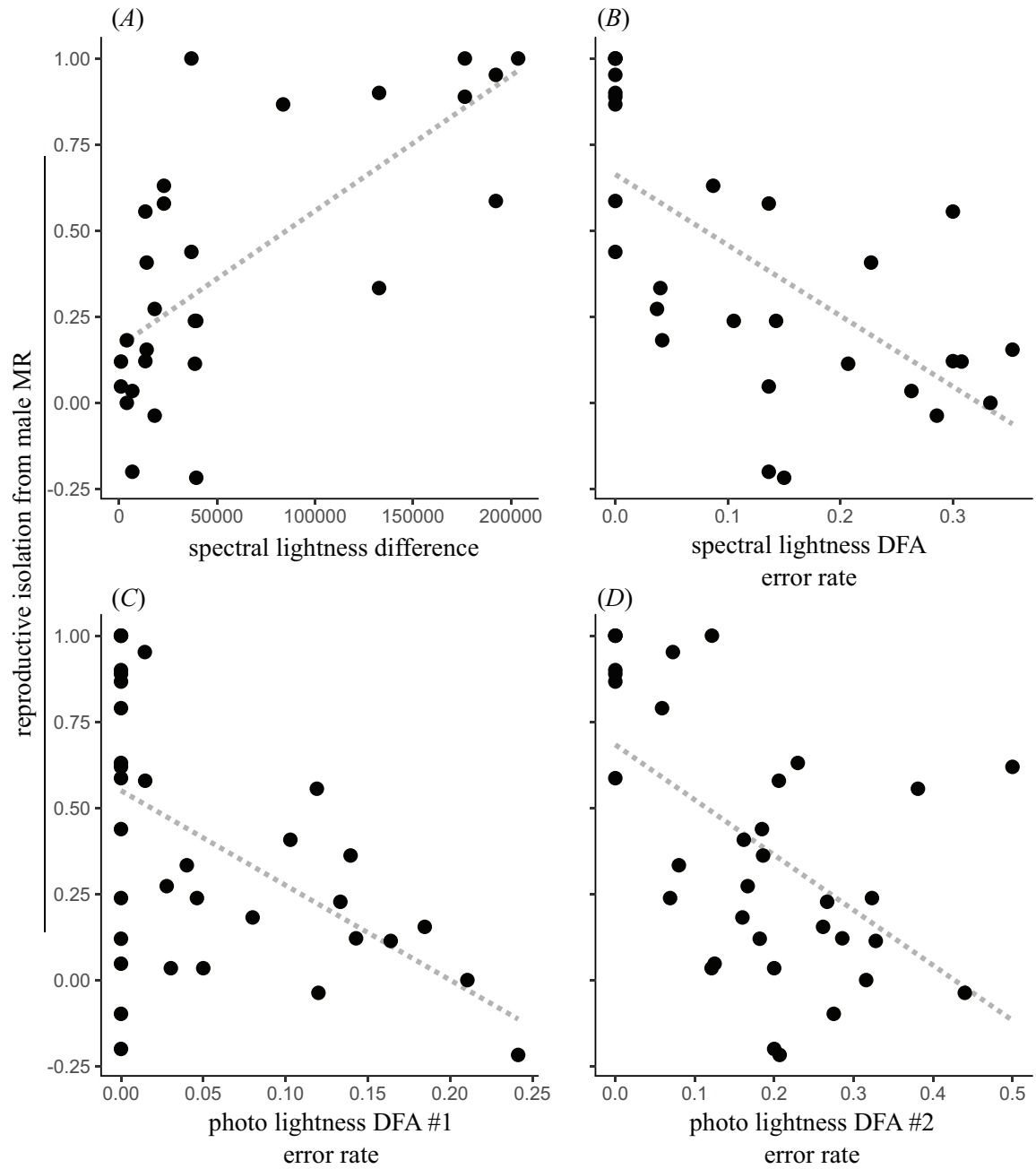


Figure A1: Using several alternative indexes comparing female wing phenotypes, we consistently find that males discriminate between conspecific and heterospecific females as a function of female wing lightness, measured as Euclidean distance in the weighted total intensity value calculated from reflectance spectra (A), the rate at which discriminant function analyses misidentify species using total intensity values from reflectance spectra (B), and the rate at which discriminant function analyses misidentify species using photographic grayscale values (C, D; see table A2 for a description of variables and table A4 for statistical analyses).

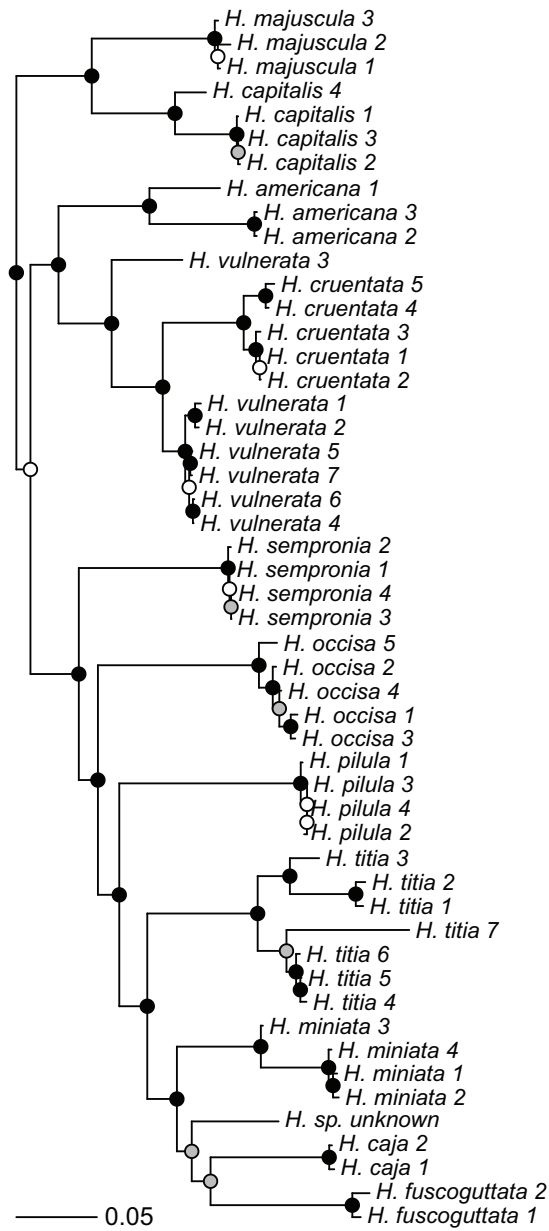


Figure A2: Maximum clade credibility tree calculated using Bayesian phylogenetic inference. Black circles indicate a mean posterior probability of >0.95 , gray circles of >0.75 and <0.95 , and white circles of <0.75 . The scale bar indicates the expected number of changes per site.

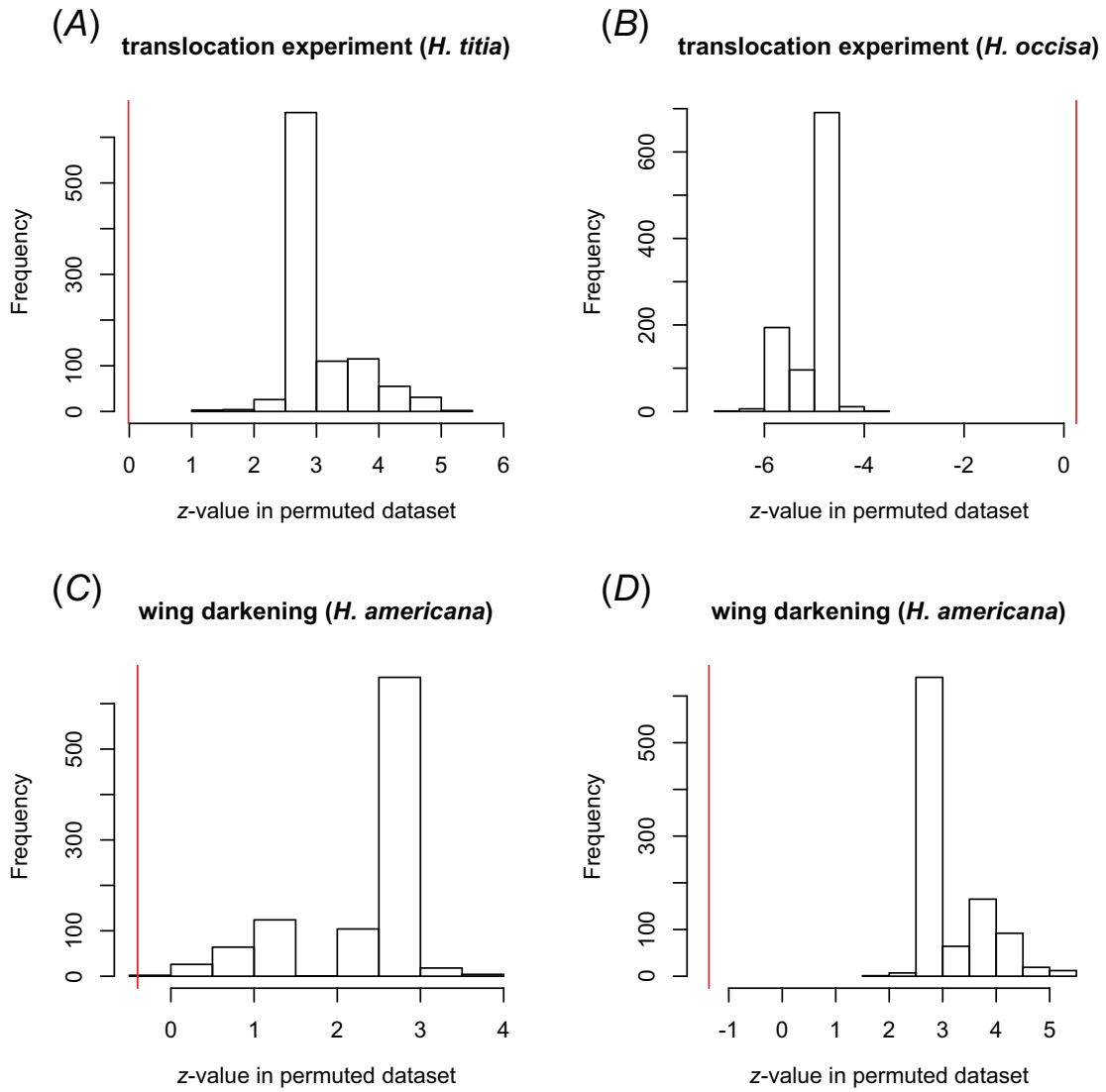


Figure A3: Null distributions of z -values for the interaction terms of models presented in table 1 and figure 3, calculated using permutation tests. In each permutation, the female treatment was shuffled for the data in allopatric sites. Panels are ordered as in figure 3. Vertical red lines correspond to the z -value in the models presented in table 1 and in every case fall outside of the null distribution.

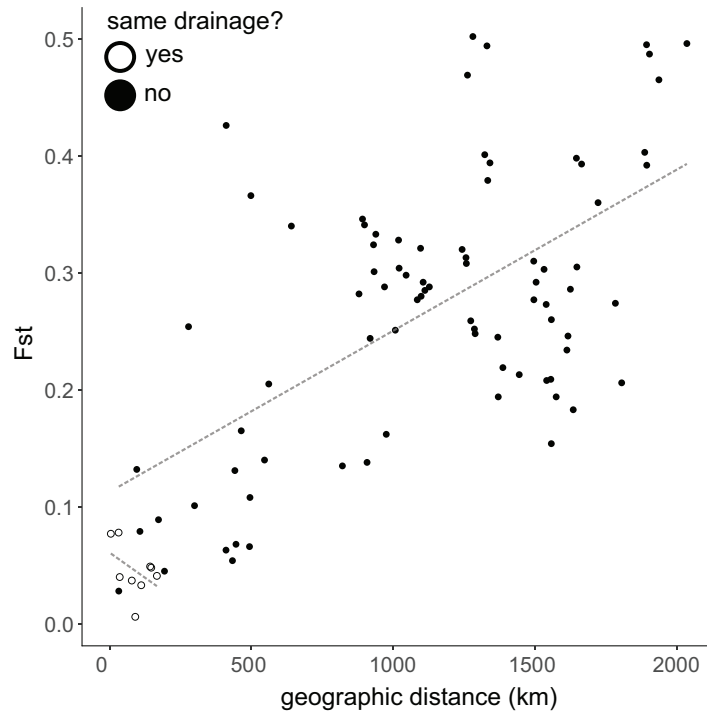


Figure A4: Isolation-by-distance relationship among populations of *Hetaerina americana*. Scatterplot of pairwise F_{ST} versus geographic distances (in kilometers) among 14 *H. americana* populations showing significant correlation between geographic and genetic distance ($r = 0.713$, Mantel test, $P = .01$). Trend lines show the predicted relationships from a linear regression including an effect of drainage.

Table A1: Study locations and *Hetaerina* species for which we measured male mate recognition (MR) at each site

Site name (abbreviation)	Species 1	Species 2	Species 3	Lat.	Long.	Analysis		
						1	2	3
Bonita Creek, USA (BC)	<i>H. americana</i>	<i>H. vulnerata</i>		32.91627	-109.49282	X		
Burr Ferry, USA (BF)	<i>H. titia</i>			31.0749	-93.495933	X	X	
Cuetzalapan, MX (CT)	<i>H. cruentata</i>	<i>H. occisa</i>		18.37100	-95.00148	X		X
Castroville, USA (CV)	<i>H. americana</i>	<i>H. titia</i>		29.33350	-98.86690	X	X	X
Laguna Escondida, MX (ES)	<i>H. sempronina</i>	<i>H. occisa</i>		18.59245	-95.08390	X	X	X
Rio Bitey, CR (ESRB)	<i>H. titia</i>	<i>H. miniata</i>		9.71961	-82.9657	X		
Golfito, CR (GO01)	<i>H. fuscoguttata</i>	<i>H. occisa</i>	<i>H. titia</i>	8.64301	-83.195277	X		
Lampasas, USA (LM)	<i>H. americana</i>			31.08271	-98.01973			X
Las Haciendas, CR (LH03)	<i>H. occisa</i>	<i>H. miniata</i>		10.98932	-85.377696	X		
San Luis, CR (MV04)	<i>H. majuscula</i>	<i>H. cruentata</i>		10.27801	-84.786277	X		
Socorro, CR (MV05)	<i>H. capitalis</i>	<i>H. cruentata</i>		10.27826	-84.818937	X		
Otapa, MX (OT)	<i>H. occisa</i>	<i>H. titia</i>		18.68339	-96.38350	X	X	
La Palma, MX (PA)	<i>H. occisa</i>	<i>H. titia</i>		18.55010	-95.06671	X	X	X
Pixquiatic, MX (PX)	<i>H. vulnerata</i>	<i>H. cruentata</i>		19.46679	-96.95018	X		
Rio Tempisquito, CR (RT02)	<i>H. occisa</i>	<i>H. capitalis</i>		10.94903	-85.511632	X		
Upper Otapa, MX (UOT) ^a	<i>H. occisa</i>	<i>H. titia</i> ^b		18.70015	-96.550277	X	X	

Note: "Analysis" columns indicate whether a site was used for analyses of variation in male MR as a function of heterospecific female wing phenotype (analysis 1), analyses of translocation experiments (analysis 2), or analyses of female wing color manipulation experiments (analysis 3).

^a This site is in the same drainage as OT.

^b A single *H. titia* male was sighted at UOT.

Table A2: Sample sizes for experiments measuring reproductive isolation due to male mate recognition (MR) in *Hetaerina* species

Site name (abbreviation), territory holder species	<i>n</i>	
	Conspecific	Heterospecific
Bonita Creek (BC):		
<i>H. americana</i>	18	18
<i>H. vulnerata</i>	18	18
Burr Ferry (BF):		
<i>H. titia</i>	15	15
Cuetzalapan (CT):		
<i>H. cruentata</i>	17	17
<i>H. occisa</i>	20	20
Castroville (CV):		
<i>H. americana</i>	24	24
<i>H. titia</i>	22	22
Laguna Escondida (ES):		
<i>H. sempronia</i>	10	10
<i>H. occisa</i>	20	20 (<i>H. sempronia</i>); 8 (<i>H. titia</i>)
Rio Bitey (ESRB):		
<i>H. titia</i>	33	33
<i>H. miniata</i>	18	18
Golfito (GO01):		
<i>H. fuscoguttata</i>	27	23 (<i>H. occisa</i>); 22 (<i>H. titia</i>)
<i>H. occisa</i>	34	30 (<i>H. fuscoguttata</i>); 26 (<i>H. titia</i>)
<i>H. titia</i>	24	21 (<i>H. fuscoguttata</i>); 19 (<i>H. occisa</i>)
Las Haciendas (LH03):		
<i>H. miniata</i>	17	17
<i>H. occisa</i>	44	44
San Luis (MV04):		
<i>H. cruentata</i>	19	19
<i>H. majuscula</i>	17	17
Socorro (MV05):		
<i>H. capitalis</i>	32	32
<i>H. cruentata</i>	34	34
Otapa (OT):		
<i>H. occisa</i>	7	7
<i>H. titia</i>	17	17
La Palma (PA):		
<i>H. occisa</i>	64 (early); 42 (late)	64 (early); 42 (late)
<i>H. titia</i>	38 (early); 24 (late)	38 (early); 24 (late)
Pixquiac (PX):		
<i>H. cruentata</i>	14	14
<i>H. vulnerata</i>	11	11
Rio Tempisquito (RT02):		
<i>H. capitalis</i>	38	38
<i>H. occisa</i>	37	37
Upper Otapa (UOT):		
<i>H. occisa</i>	13	13

Note: There was no relationship between the isolation index used in subsequent analyses and the number of conspecific trials (Spearman's rank correlation, $\rho = -0.15$, $P = .38$) or heterospecific trials (Spearman's rank correlation, $\rho = -0.24$, $P = .17$).

Table A3: Indexes of pairwise comparisons of female wing lightness used in analyses

Index	Description
Photo lightness difference	Euclidean distance in population mean of sum of grayscale values (calculated with RGB Measure function in ImageJ MBF package; Collins 2007; Schneider et al. 2012) across all four wing patches (basal, distal, hindwing, and forewing)
Photo lightness overlap	Proportional overlap of density curves calculated (using overlapping package in R; Pastore 2017) from individual-level data of sum of grayscale values across all four wing patches (basal, distal, hindwing, and forewing)
Photo lightness DFA no. 1 error rate	Proportion of heterospecific females misidentified as conspecific females in a discriminant function analysis conducted (using lda function in R MASS package; Venables and Ripley 2002) with individual-level data from all three RGB channels across all four wing patches (12 measurements per individual)
Photo lightness DFA no. 2 error rate	Proportion of heterospecific females misidentified as conspecific females in discriminant function analysis conducted with individual-level data from grayscale value across all four wing patches (four measurements per individual)
Spectral lightness difference	Euclidean distance in population mean of midpatch weighted total intensity value (calculated using $L_{total} = .1 L_{base} + .8 L_{middle} + .1 L_{tip}$ and summing both wings) from reflectance spectra across all six wing scans (basal, mid, and tip of hindwing and forewing)
Spectral lightness DFA error rate	Proportion of heterospecific females misidentified as conspecific females in discriminant function analysis conducted with individual-level data from total intensity value across all six wing scans (basal, mid, and tip of hindwing and forewing, totaling six measurements per individual)

Note: DFA = discriminant function analysis.

Table A4: Collection locations and GenBank accession numbers for new specimens included in updated *Hetaerina* phylogeny

Specimen	Collection location	Lat., long.	Locus									
			1	2	3	4	5	6	7	8		
<i>H. caja</i> 1	Rio Palo Seco, Costa Rica	9.53508, -84.27901		MK238651	MK238667			MK243636	MK243672			MK238645
<i>H. caja</i> 2	Rio Desjarretado, Costa Rica	10.30183, -85.03687		MK238650	MK238666			MK243635	MK243663			MK238644
<i>H. cruentata</i> 4	Cacao Sector, Costa Rica	10.92329, -85.46551	MK238673		MK238665		MK243657	MK243645				MK238636
<i>H. cruentata</i> 5	Quebrada Alondra, Costa Rica	10.28359, -84.79358					MK243658	MK243646	MK243658			
<i>H. fuscoguttata</i> 1	Rio Bonito, Costa Rica	8.70227, -83.21365			MK238669		MK243654	MK243638				MK238643
<i>H. fuscoguttata</i> 2	Quebrada Bonita, Costa Rica	9.77400, -84.60319		MK238648				MK243637	MK243664	MK243675		
<i>H. majuscula</i> 1	Rio San Luis	10.27801, -84.78628					MK243650		MK243670			MK238639
<i>H. majuscula</i> 2	Rio San Luis	10.27801, -84.78628										MK238637
<i>H. majuscula</i> 3	Quebrada Pedegral, Costa Rica	10.92609, -85.47166			MK238661		MK243651		MK243671			MK238638
<i>H. occisa</i> 5	Quebrada Aserradero, Costa Rica	10.898356, -85.56385					MK243648		MK243665			MK238631
<i>H. sp.</i> unknown	Tiputini, Ecuador	-63740, -76.14974			MK238668		MK243647					MK238646
<i>H. titia</i> 5	Rio Armeria, Mexico	18.95001, -103.93351			MK238660			MK243640	MK243667			MK238642
<i>H. titia</i> 6	Rio Armeria, Mexico	18.95001, -103.93351			MK238659		MK243649		MK243661			MK238641
<i>H. titia</i> 7	Rio Tarcolitos	9.75709, 84.61775					MK243659	MK243639	MK243659			MK238640
<i>H. vulnerata</i> 4	Bonita Creek, AZ	32.91627, -109.49282			MK238662		MK243655	MK243644	MK243668			MK238634
<i>H. vulnerata</i> 5	Cave Creek, AZ	31.86238, -109.243667			MK238663		MK243652	MK243641	MK243662			MK238633
<i>H. vulnerata</i> 6	Rio Palo Seco, Costa Rica	9.53508, -84.27901			MK238664		MK243656	MK243643	MK243669			MK238635
<i>H. vulnerata</i> 7	Cave Creek, AZ	31.86238, -109.243667			MK238658		MK243653	MK243642	MK243674			MK238632

Note: For additional details on loci and primers, see Drury et al. (2015b). Locus 1 = cytochrome oxidase I; locus 2 = 16s rRNA (partial); locus 3 = 12s rRNA (partial), tRNA-valine (complete), 16s rRNA (partial); locus 4 = 16s rRNA (partial), tRNA-leucine (complete), NADH dehydrogenase I (partial); locus 5 = elongation factor α (partial); locus 6 = histone 3; locus 7 = tubulin alpha; locus 8 = 18s and 28s rRNA (partial), 5.8s rRNA (complete).

Table A5: Correlations between reproductive isolation indexes and species comparisons of female wing coloration

Index	Empirical mean $\rho \pm$ SD	Phylogenetic mean $\rho \pm$ SD		<i>P</i>	
		BM	OU	BM	OU
Photo lightness difference	.54 \pm .08	.02 \pm .30	.01 \pm .31	<.001	<.001
Photo lightness overlap	-.64 \pm .07	-.16 \pm .23	-.18 \pm .24	<.001	<.001
Photo lightness DFA no. 1 error rate	-.52	.01 \pm .15	.01 \pm .15	<.001	<.001
Photo lightness DFA no. 2 error rate	-.59	.03 \pm .17	.02 \pm .17	<.001	<.001
Spectral lightness difference	.71 \pm .08	.02 \pm .31	.01 \pm .31	<.001	<.001
Spectral lightness DFA error rate	-.75	-.04 \pm .22	-.03 \pm .22	<.001	<.001

Note: Empirical estimates of ρ statistics from Spearman’s correlations tested against null ρ distributions calculated from phylogenetically simulated data sets. *P* values are from one-sample *t*-tests. Standard deviations are presented for empirical data sets where we conducted randomization tests to account for pairwise analyses (see appendix). DFA = discriminant function analysis.

Table A6: Population abbreviations, site description, geographic information, and number of genetic samples per population for microsatellite analyses of *Hetaerina americana*

Population code	Site description	Lat.	Long.	<i>N</i>
P001	Armeria, Mexico	18.95002	-103.934	20
P002	Tehuixtla, Mexico	18.54733	-99.2695	9
P006	Rio Cebadilla, Mexico	19.6334	-104.483	9
P007	Bridge to Autlan, Mexico	19.85082	-104.283	7
P008	Rio Limon, Mexico	21.36674	-104.617	14
P009	San Luis Potosi, Mexico	22.05957	-100.492	8
P011	Gila River, AZ	32.88384	-109.517	9
P012	Bonita Creek, AZ	32.90923	-109.487	6
P013	San Francisco River, AZ	33.13293	-109.282	7
P014	Tularosa River, NM	33.89524	-108.506	7
P015	Rio Grande, NM	35.80315	-106.194	8
P016	Roosevelt, TX	30.49153	-100.066	8
P017	New Braunfels, TX	29.87414	-98.4892	8
P018	Guadalupe River, TX	30.06675	-99.2669	11

Table A7: Linear regression fit of F_{ST} with geographic distance for a sample of 14 populations of *Hetaerina americana* (table A6), accounting for whether populations are in the same or different drainage

Model term	Est.	SD	<i>t</i> -value	<i>P</i>
Intercept	.11	.024	4.71	<.001
Distance (km)	.00014	.000019	7.07	<.001
Drainage (same)	-.08	.037	-2.15	.035

Table A8: Geographic distances and predicted levels of genetic isolation between sites included in tests of reproductive character displacement

Comparison	Male species	Distance (km)	Same drainage	Analysis		F_{ST} (predicted)	Level of isolation ^a
				2	3		
BF, CV	<i>Hetaerina titia</i>	551.9	No	X		.189	Great
PA, ES	<i>Hetaerina occisa</i>	5.0	No	X	X	.114	Moderate
OT, UOT	<i>H. occisa</i>	17.7	Yes	X		.036	Low
CV, LM	<i>Hetaerina americana</i>	210.4	No		X	.142	Moderate
PA, CT	<i>H. occisa</i>	21.0	No		X	.116	Moderate

Note: Predictions were derived from a linear regression of the observed F_{ST} values and distance from *H. americana* populations (table A7; fig. A4). See table A1 for site abbreviations and analysis numbers.

^a See Hartl et al. (1997).

Table A9: Analyses of *Hetaerina occisa* male sexual responses toward tethered conspecific and heterospecific females in sympatry and allopatry, excluding the Otapa and Upper Otapa comparison, which took place within the same drainage

Term	Est.	SE	z-value	P
Intercept	3.65	1.47	2.49	.013
Female species (<i>Hetaerina titia</i>)	-7.27	1.82	-4.0	<.001
Site type (sympatry)	.03	1.40	.02	.98
Female species × site type	-.11	1.66	-.06	.95

Note: Translocation experiment with 50 male *H. occisa* and logistic regression models fit using bayesglm in R.